

Seismic Performance of a Dolphin-Type Berth Structure under Post-Fire Conditions

Abbas Rezaeian¹
Farhad Hosseinlou²
Abdulameer Qasim Hasan³
Nazar yaseen Kuioon⁴

Abstract

A large number of fires occur in offshore structures as a result of oil spill or earthquake. A potential but rarely examined risk is the sequential happening of fires and earthquakes. The high ignition temperature can have serious structural influences on the seismic behavior of dolphin-type berth structure. The fire induced structural effects on the seismic performance of Dolphin structure is not well unstated, but may be critical in the occurrence of aftershocks and/or future ground excitations. Considering the irreparable consequences of reducing the seismic performance of fixed marine structures under post-fire conditions, it is vital for engineers to better understand post- fire earthquake hazards in Dolphin structure. The current manuscript presents a numerical investigation to examine the influence of post-fire conditions on the seismic behavior of dolphin-type berth structure. the main goal of this paper is to investigate the effects of fire on the seismic response of the structure. In order to better investigate the effects of temperature increase on the performance of the structure, fire is applied in the first stage near the water surface and in the second stage to the berth deck. The ABAQUS software package is utilized to model and solve the problem.

Keywords: Fixed marine structures, Seismic Performance, post- fire earthquake, Dolphin-type berth.

Received: 17 December 2023; Accepted: 20 January 2024

1. Introduction

The spread of offshore oil platforms across seas and oceans is not a coincidence, rather it reflects the human need for this energy source. These platforms are vulnerable to certain

¹Associate Professor, Faculty of civil engineering and architecture, Shahid Chamran University of Ahvaz, Ahvaz, Iran.

² Assistant Professor, Faculty of civil engineering and architecture, Shahid Chamran University of Ahvaz, Ahvaz, Iran. Email: F.hosseinlou@scu.ac.ir (Corresponding author)

³ Assistant Professor, Engineering technical college, Southern technical university, Basra, Iraq.

⁴ Graduate Student, Civil Engineering Department, Shahid Chamran University of Ahvaz, Ahvaz, Iran.

circumstances (earthquakes and fires). Therefore, in order to avoid significant material and human losses, we must consider the effects of these loads in the design and implementation/ or performance of marine structures. Hereof, more study based on extensive tests and simulations is urgently needed to establish a profound understanding of the most critical characteristics that determine the fire and earthquake resistance. Many studies have been conducted in the field of seismic behavior of fixed marine structures. In the following, some of them are mentioned as instances.

Vazirizade et al. [1] developed a new approach for assessing the dependability of dynamically loaded offshore platforms using jacket-type moorings in the time domain (seismic and wave). To collect risk data, they employed the multiple finite element-based investigations. They considered around 200 deterministic trials and 10,000 Monte Carlo simulations to establish the platform's strength and serviceability performance functions' failure probability. In terms of strength and serviceability limits, the coefficient of variations was larger for seismic loading than for wave loading. In this circumstance, anticipating the seismic loading was more challenging than predicting the wave loading. Hosseini et al. [2] assessed the seismic response of a jacket platform (SPD9) via the idealized model under an earthquake acceleration. They utilized a scaled hydro-elastic model of a jacket platform (SPD9) for the experimental evaluation of a simplified technique using an upgraded simple dynamic model. Hereof, to improve a baseline FE model, the numerical model was enhanced using experimental data and a model reduction strategy was also applied in the process of updating the model. The dynamic properties of the upgraded simplified and ideal model were calculated via the updated model attributes. The effects of increased deck weight, corrosion, and marine growths were also investigated. Zheng et al. [3] investigated the seismic behavior of corroded steel columns in the offshore air environment based on both experimental and computational methods. First, six steel columns and 48 tensile coupons were subjected to a series of indoor artificial environment accelerated tests. When the axial compression ratio was increased from 0.2 to 0.4, the plastic rotation, cumulative energy dissipation, ductility coefficient, and maximum load all dropped by 26.97%, 18.60%, 10.63%, and 10.68%, respectively. They demonstrated that for seismic design of steel columns, the application of a proper axial compression ratio is critical in structural engineering. Asgarian et al. [4] studied the performance and failure modes of a newly designed platform. To investigate the effects of soil conditions on the platform's behavior and failure modes, they selected two unique soil profiles called SC1 (weak soil) and SC2 (strong soil). They concluded that due to the high indeterminacy in the construction of the jacket, the strength proportionality between the foundation and the platform's jacket section leads to enhance the platform performance and helps to prevent the immature failure. Furthermore, the stronger soil profiles cause the entire platform to be stiffer and stronger, yet the failure tendency remains unchanged. Also, increasing the moment of inertia (strength) of the piles can cause the braces to buckle before the piles fail. Yang et al. [5] evaluated the seismic behavior of fixed marine structures through time-variant zonal corrosion model. Based on corrosion characteristics, they simulated the different time-variant corrosion models. The planned time-variant zonal can well reflect the features of the non-uniform spatio-temporal distribution of corrosion of aging jacket structures. Som and Das [6] estimated vibration performance of fixed marine structures via decentralized sliding mode technique. They considered the effect of linearization of drag force. The results indicated that both controlled and uncontrolled response increase when the jacket is analyzed via linearized drag force. They also found that the positions and the number of MR dampers have quite important effect on the performance of the controller. Kavand et al. [7] assessed the seismic performance of a dolphin-type berth under liquefaction induced lateral spreading. They considered two different numerical methods to

simulate the performance of the marine dolphin under lateral spreading. Their proposed method included a series of simple displacement-based analyses utilizing nonlinear p-y springs. Finally, a comprehensive parametric investigation on the confirmed FE model exposed that the relative density of soil and the amplitude of base excitation can deeply affect the induced bending moments in piles. Kaynia [8] presented a robust computational model for monopole-soil interactions in layered soil to forecast both rotational kinematic and horizontal responses at the monopile's head (seabed level). According to the investigations, seismic soil-structure interaction analyses that include kinematic interaction result in a bigger tower response and more bending moments for all soil profiles considered. Kinematic interaction appears more in stronger soils. The influence of kinematic interaction increases with frequency as the monopile rotates. As a result, the impact is highest when the tower is governed by the second mode.

In addition to seismic loads, the fixed marine structures (especially dolphin-type berth) are also exposed to fire conditions. The simulation of fixed marine structures subject to fire loads contains the solution of a fluid-thermo-mechanical problem [9, 10]. Three main physical features are involved in the related problem, i.e., fire development, heat transfer and structural response [11]. At present, many works have been accomplished in the field of material mechanical behavior at high temperature [12, 13], and some studies have been done to evaluate the structural behavior of tubular joints and CFST columns subjected to axial loadings at fire-induced elevated temperatures [14-18].

Nevertheless, the above investigations mainly focus on the material mechanical behavior at high temperature. Also, existing works only assessed the behavior of part of the fixed marine structures (such as joints and columns) under fire. In connection with the investigation of the seismic performance of the entire dolphin-type berth structure that has already been subjected to fire, no case study has been conducted. As stated above, to conquer the shortage of the fire safety evaluation schemes of fixed marine structures (especially dolphin-type berth), it is required to examine the actual seismic behavior of steel offshore structures after exposure to fire. The goal of this manuscript is to evaluate the seismic response of the dolphin-type berth structure after exposure to various fire scenarios. For this purpose, first the response of the dolphin-type berth structure exposed to fire load is obtained. Then, the considered structure that experienced the fire load is subjected to an earthquake record. Finally, the response of the studied structure under primary fire and secondary earthquake loads is compared with the response of the studied structure under fire. In better words, it can be said that the main goal of this paper is to investigate the effects of fire on the seismic response of the structure. In order to better investigate the effects of temperature increase on the performance of the structure, fire is applied in the first stage near the water surface and in the second stage to the berth deck. The ABAQUS software package is utilized to model and solve the problem. To validate the current research, a laboratory steel model under fire load is selected [19]. This laboratory work is simulated in ABAQUS software and the gained numerical results are compared with the laboratory results. For each case of a hydrocarbon fire, the study investigated the effect of fire location on displacements in the deck of platform and the displacements and shear stress along with the columns and the steel piles.

2. FE simulation and Verification

2.1. Structure Modeling

The dolphin's structure is divided into two sections: the superstructure, which contains 492 steel beams, and the deck slab, which has an I-cross shape. The deck slab also includes tube beams of various sizes. The substructure, or deep foundation, is the second portion (piles). The dolphin is made up of eight steel tube pipe piles with a length of 40 meters and an outside diameter of 1000 millimeters

and a wall thickness of 12.5 millimeters. The components and dimensions of the dolphin are shown in Figure (1).

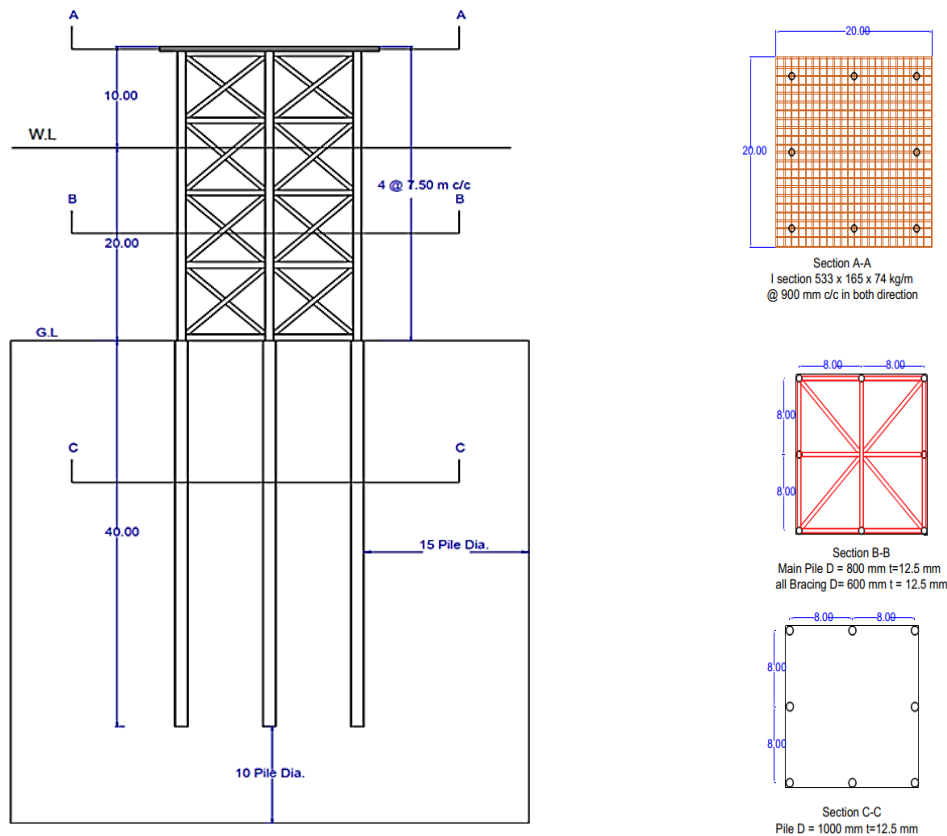


Figure (1). Structure details of AL-Amaya berthing dolphin

Table (1) shows the details of all beams and piles. The steel modulus of elasticity is 210 GPa and Poisson's ratio equals to 0.3. Steel unit weight of 7850 kg/m^3 is used for all sections. The ABAQUS finite element (FE) package employed to model and solve the problem. The FE model of AL-Amaya berthing dolphin is revealed in Figure (2).

Table (1). Structure Section details of AL-Amaya berthing dolphin

Type	Section	Dimension
Main Pile	Tube	D= 800 mm, t= 12.5 mm
All Bracing	Tube	D= 600 mm, t= 12.5 mm
Pile	Tube	D= 1000 mm, t= 12.5 mm
Deck Girder	I-section	H=533 mm, B = 165 mm, t = 74 mm

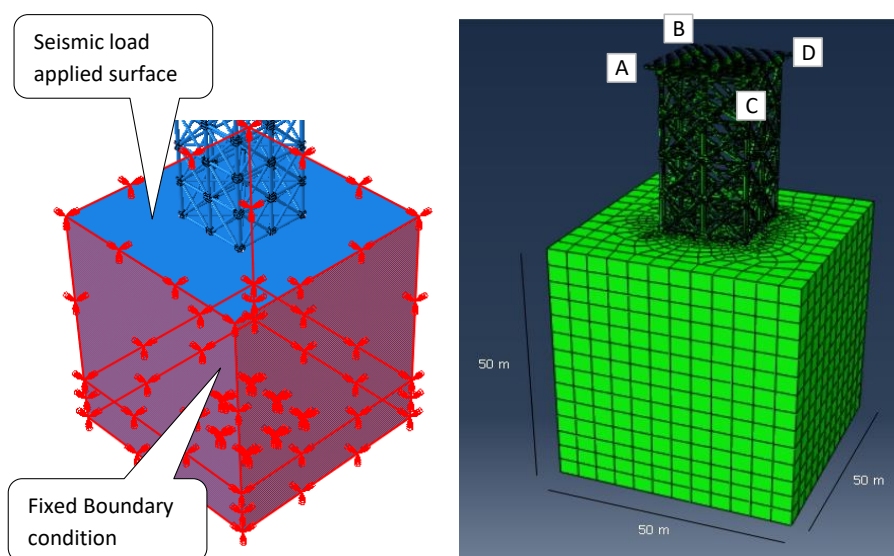


Figure (2). FE Model of AL-Amaya berthing dolphin

The soil is modeled as a cube with dimensions of $50 \times 50 \times 50 \text{ (m}^3\text{)}$. The elastic-plastic Mohr-Column model is utilized to represent the behavior of clay soil in the dynamic analysis under seismic load. The properties of soil are given in Table (2). The piles are assumed the embedded element in the soil. It is assumed that the bond between the interaction of the soil and piles is fully connected. For this purpose, the "Tie-Constrain" has been applied in the modeling process. A 20-node block with quadratic displacements (C3D20) is considered to model the elements of steel frame and soil and each node has three displacements in three directions x, y, and z. These features make modeling problems with curved borders easier and more precise [20].

Table (2). Specific material of the soil

Soil type	Density (Kg/m ³)	Young modulus (MPa)	Poisson ratio	Cohesive	Angle of friction
Clay	1800	40	0.35	44	10

2.2. Fire loading and the behavior of steel

The petroleum fire load happens as a result of the explosion of one of the oil transport pipelines, or in other situations as a result of the platform being exposed to an earthquake or the crash of ships on the platform. To avoid losses during these fires, these loads must be taken into account during the design stage. The design techniques for the fire on a platform are detailed in section C18.6.3 of API RP 2A 22nd edition. These calculations concern the maximum permissible temperature of steel for a given strain in order to maintain platform structural uniformity (the zone method). Still, this method is acceptable for the fire protection design. The maximum temperature and period of fires offshore are the Fire Protection Engineers' responsibility to determine in offshore structures. Generally, the API RP 2A 22nd edition could be utilized as a design guidelines standard, and it will be good to follow the recommendations of an engineer familiar with fire protection. Section 5 of DNV-RP-C204 also discusses the fire loads for oil platforms. The designer should be able to provide the

certification that the fire load analyses on the platform were conducted out considering either of the BSEE / BOEM codes. The standard fire curve and how steel performs at high temperatures according to Euro-code are covered in this sub-section. The standard temperature-time curve, also known as the nominal temperature curve, is a typical manner of representing the temperature growth due to the fire in an enclosure. This curve is also known as the "834-ISO" curve. Figure (3) depicts the time-temperature relationship. The structural resilience of a member in the fire circumstances is evaluated utilizing the time-temperature relationship.

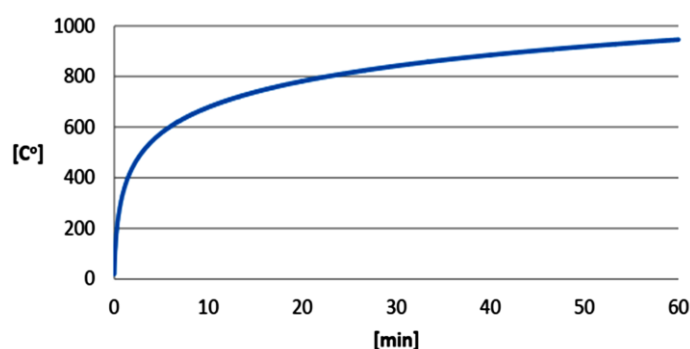


Figure (3). Standard fire curve (ISO-834)

The point at which the steel begins to yield, or the point at which the stress strain curve leaves from the elastic area, is a common way to measure steel strength. When there is no well-defined elastic limit or ultimate strength point for a given steel, the yield point is chosen at the point where the steel has a remaining elongation of 0.2% after unloading. Also, there is some residual resistance in the steel after reaching the elastic limit, although this is rarely taken into account due to the difficulty of predicting the steel's behavior in the plastic zone and to be on the "safe side."

Other phenomena in the compressive region of the steel, such as local or global buckling, frequently have a bigger impact on the behavior of a steel member than the residual resistance in the tensional part of the cross-section after the elastic limit. EN-1993-1-2 describes three basic structural behavior parameters of steel that are lowered at high temperatures [21]. The steel yield strength reduction, the elastic limit reduction, and the proportional limit reduction are these metrics. More details can be found in Buchanan [22]. EN-1993-1-2 (European Committee for Standardization) contains the rules for calculating steel behavior at increased temperatures [21]. In the cooling stage, the specimen was cooled naturally by air-cooling via convection, as shown in Figure (4).

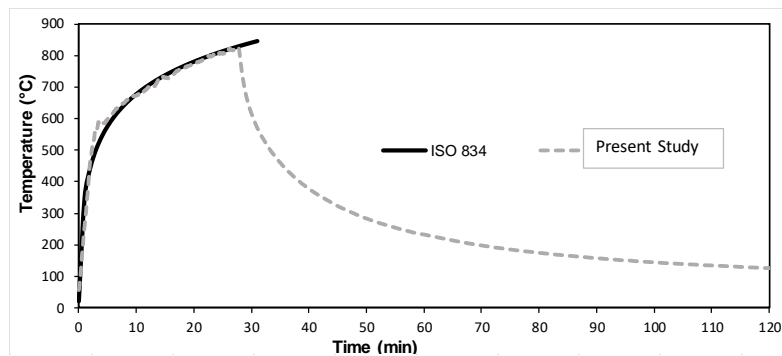


Figure (4). The temperature-time curve of cooling stage [22]

2.3. Earthquake loading

The ground motion record considered in this study is obtained from Peer Ground Motion Database (PEER-Center). The seismic acceleration record is for El-Centro at MAY 18 1940, as exposed in Figure (5). The original ground motion record has been scaled to fit each of the design response spectrum curves established in Figure 5. The design response spectrum curve (S_a) for Baghdad city, Iraq is revealed in Figure (6), which is produced based on the spectral acceleration (S_a) value that corresponds to the fundamental period of the building, according to UBC 1997, IBC 2012, and Iraqi seismic code (ISC) 2017. For the considered record, the acceleration values are applied to the buildings for 39 seconds for each 0.005 second time interval. The dynamic implicit analysis has been performed to evaluate the seismic effect on the bottom surface of the soil in x-direction.

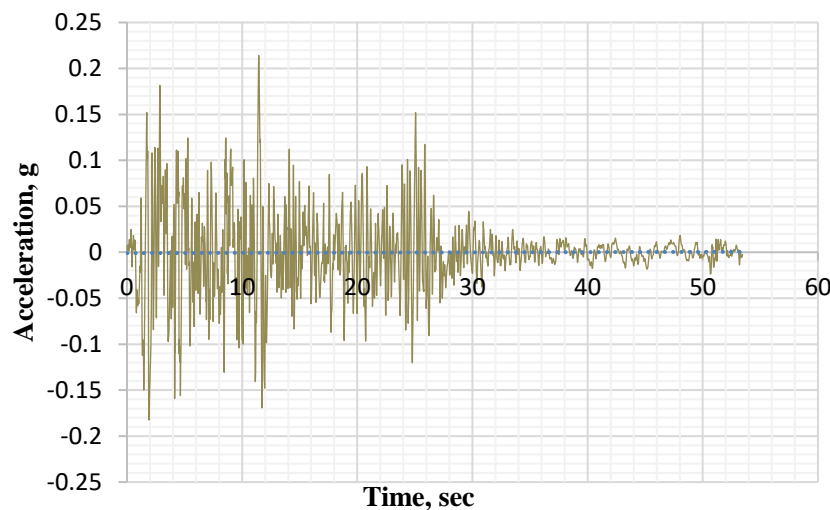


Figure (5). El-Centro Seismic Wave at MAY 18, 1940.

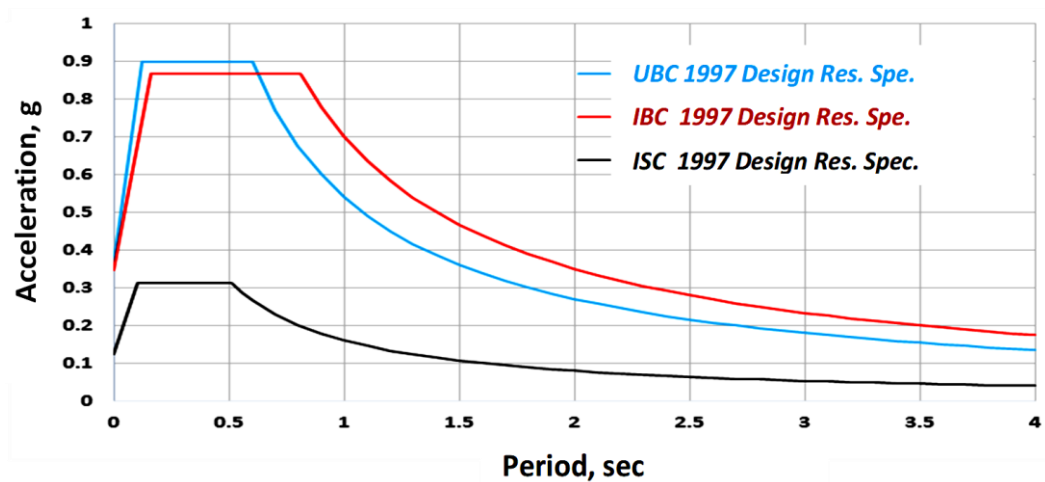
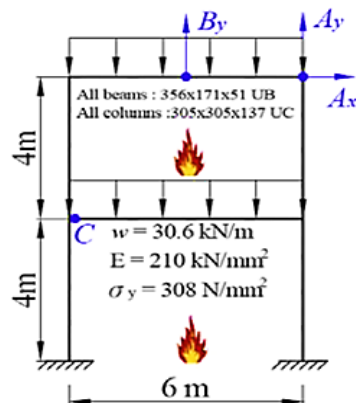


Figure (6). Design response spectrum curve for Baghdad area defined in according with UBC 1997, IBC 2012 and ISC 2017.

2.4. Validation

The two-story, one-span frame model is a stationary frame made up of a $365 \times 171 \times 51$ UB beam and a $305 \times 305 \times 137$ UC column (Lien et al., 2010). The considered model is subjected to an evenly distributed load on both the upper and lower beams, as revealed in the Figure (7). For the frame material, the European code 1993 (part 1-2) is utilized. To get more details about the specifications of the frame model and types of loading, refer to the work of Lien et al., 2010. The modeling and loading process has been done in ABAQUS software. Fire analysis (temperature loading) and earthquake load under dynamic implicit analysis are done. So, El-Centro earthquake 1940 was used to apply seismic effect to the model. Figure 8 depicts the displacement contour line under static and heat loading, as well as a comparison of the FE analysis and experimental results. Figure 9 also depicts the displacement contour line under static, heat and earthquake loading, as well as a comparison of the FE analysis and experimental results. All comparisons with experimental results yielded positive results.

A)



B)

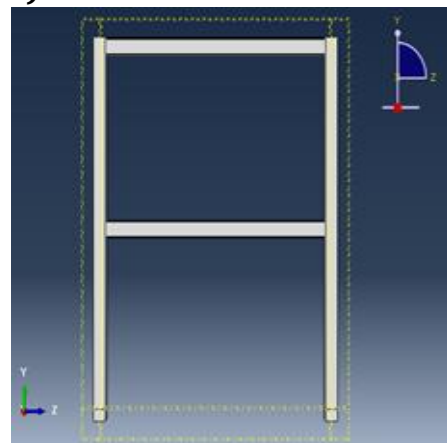


Figure (7). (A): Tested frame details (Lien et al., 2010) and (B) FE model (current study)

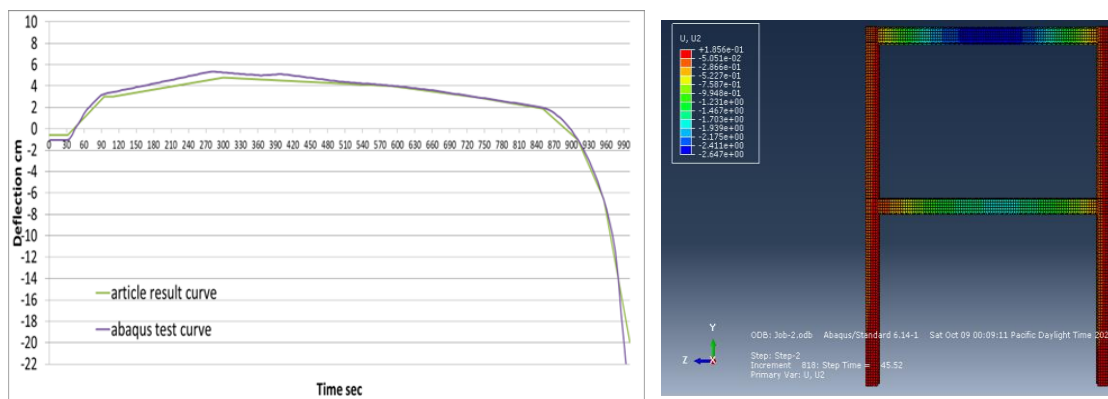


Figure (8). Displacement contour line under static and heat loading

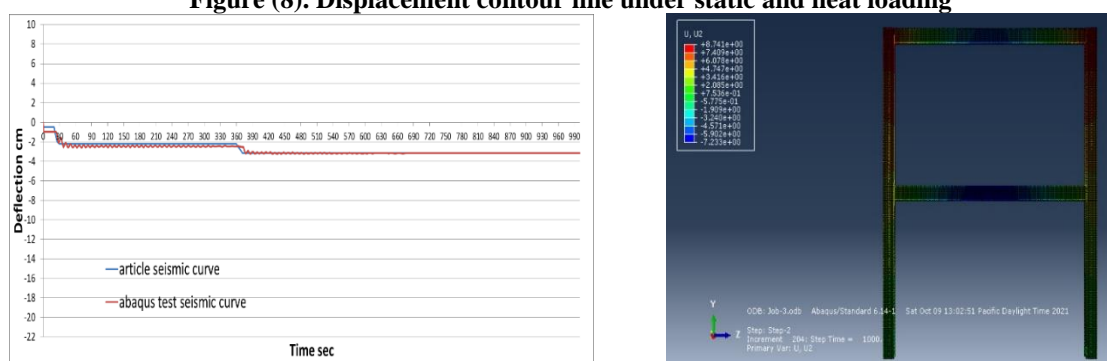


Figure (9). Displacement contour line under static, heat and earthquake loading

3. Results and Discussion

This work discussed the response of a steel offshore platforms (AL-Amaya dolphin-type berth) that were previously exposed to hydrocarbon fire conditions and then were subjected to seismic loads. After the fire, the desired berth will be repaired. Then the operating conditions of the repaired berth are provided. The aim of this manuscript is to investigate the most dangerous situation of seismic resistance of the berth structure after the fire impacts. Hereof, the fire is applied in two locations: A) near the water surface and B) the berth deck. Finally, the seismic capacity of the dolphin-type berth is evaluated under the El Centro earthquake record.

3.1. Applying fire to the dolphin-type berth

3.1.1. The structural response of the deck under fire

As previously stated, the response of the dolphin structure under the effect of fire on the deck (first scenario) and on the water surface (second scenario) is examined in this paper. By applying the first scenario, the displacement of deck is gained at two distinct points (i.e., the center/ or middle and the corner of the berth deck). Figure 10(A) displays the response of the dolphin structure (deck displacement) under the first scenario at the two mentioned points. The displacement obtained from the middle of the deck is in the opposite direction of the displacement acquired from the corner of the deck. This indicates that the steel has entered the flexibility stage under fire. Also, Figure 10(B) depicts the response of the dolphin structure (deck displacement) acquired from the deck midpoint and the deck corner under the second scenario. In this situation, the responses obtained from two points are in the same direction.

The gained displacement of deck midpoint is about 13% more than the gained displacement of deck corner. The maximum displacement calculated in the second scenario (Applying fire on the water surface) is 57% higher than the maximum displacement determined in the first scenario (Applying fire on the topside of the structure/ or deck).

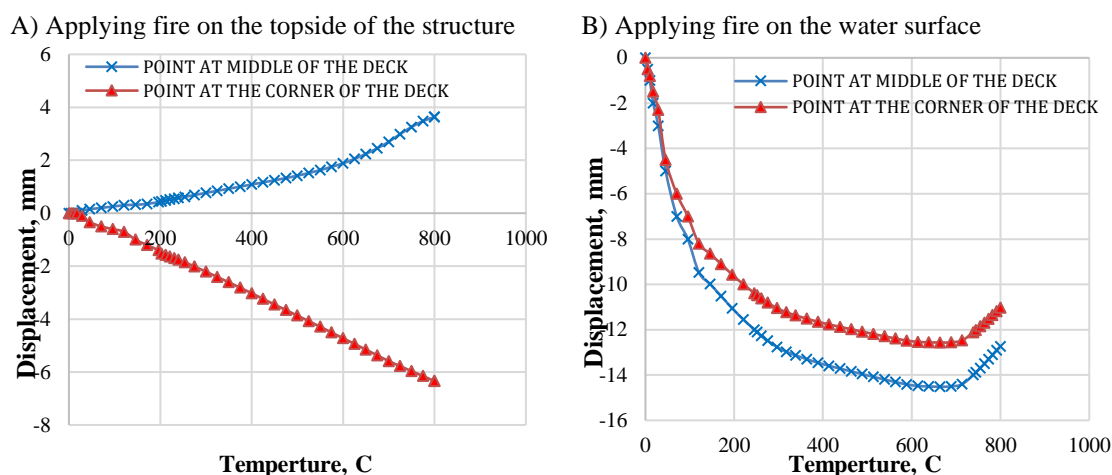


Figure (10). Displacement-temperature curve of the dolphin-type berth deck: A) first scenario and B) second scenario

3.1.2. The structural response of the column under fire

In this sub-section, the structural response (displacement and shear stress) of the columns from the ground level to the topside of the structure is examined under the first and second scenarios of fire loading. In this analysis, the four corner columns are marked with A, B, C and D. Figures 11 and 12 illustrate the structural response of the four studied columns under both scenarios. In examining the effect of the location of the fire on the response of the columns, it can be stated that the effect of fire in the first scenario is less than the effect of fire in the second scenario.

In this regard, the displacement of the considered columns under the second scenario is about 45% more than the displacement of columns under the first scenario. It can be said that the fire is applied to the place of possible buckling of the columns, which is the critical area of the columns. In each fire loading scenario, the displacement of examined columns has occurred in two opposite directions. This means that the steel members thermal expansion is outward. Also, the shear stress of the examined columns under the second scenario is about 28% more than the shear stress of columns under the first scenario.

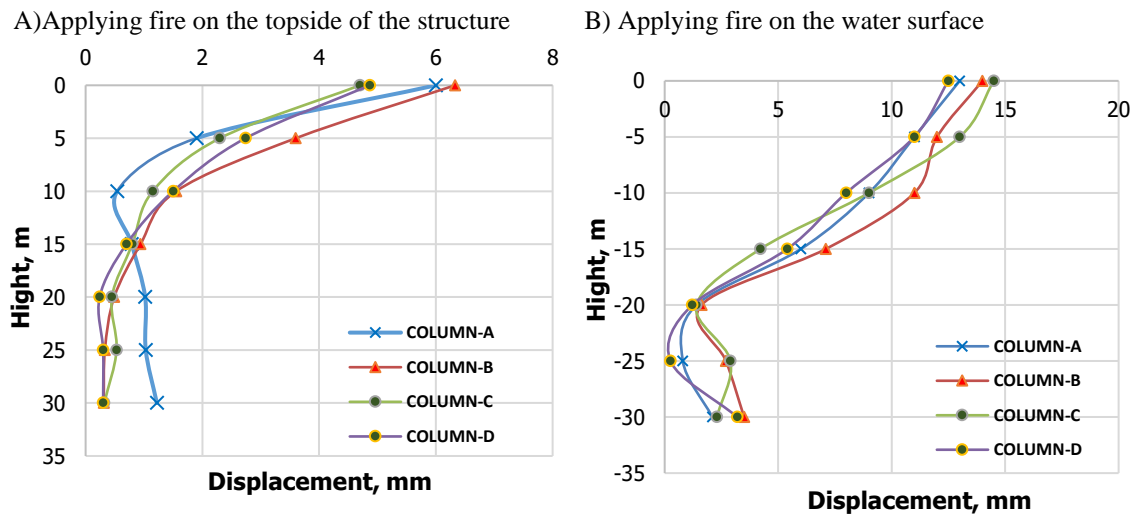


Figure (11). Column displacement of dolphin-type berth: A) first scenario and B) second scenario

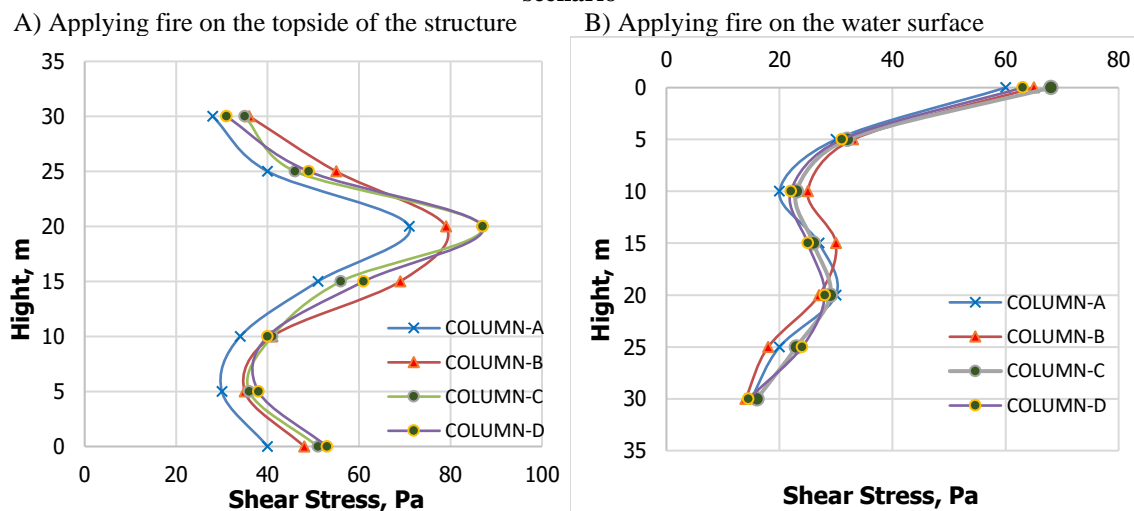


Figure (12). Shear stress of columns under the fire: A) first scenario and B) second scenario

3.2. Applying earthquake record to the dolphin-type berth

In this sub-section, a one-way acceleration (x-direction) seismic load (El Centro earthquake record) is applied to the dolphin-type berth. In the next step, the seismic response of steel berth members such as deck, columns and piles are evaluated.

3.2.1. Seismic displacement of berth deck

The seismic displacements are calculated utilizing two points in the center and corner of berth deck. The seismic response of the steel dolphin-type berth in the form of deck displacement is given in Figure 13. Given that the dolphin steel structure has high stiffness (rigid performance) and the seismic load has no effect on the material properties, there is no substantial variation in displacements when applying the seismic load to the structure.

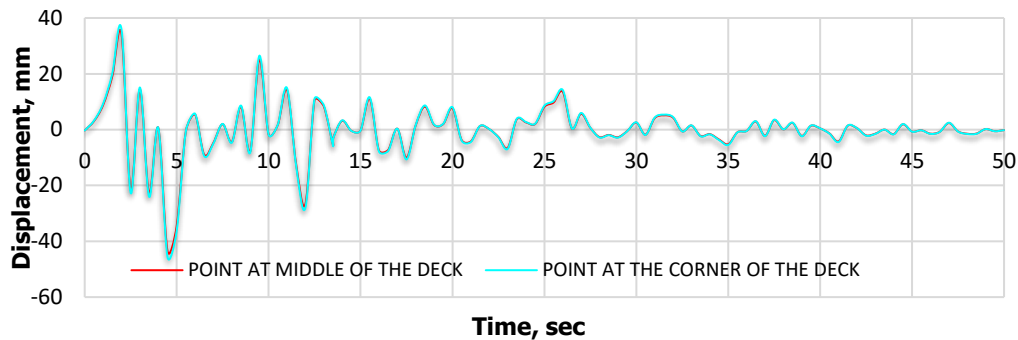


Figure (13). Seismic displacement of berth deck

3.2.2. Seismic behavior of the columns

In this sub-section, the seismic behavior (displacement and shear stress) of four columns under the applied earthquake load has been investigated. The results are presented in Figure 14. According to Figure 14A, the seismic displacement of all the columns is distinct and happened in the same direction. The effect of the seismic load on the shear stress of Dolphin structure columns is also revealed in Figures 14B. Because of the variance in seismic wave intensity, all columns have different shear stress values. It's also possible to view the shear stress for all columns in the same direction because the seismic load moves in one direction.

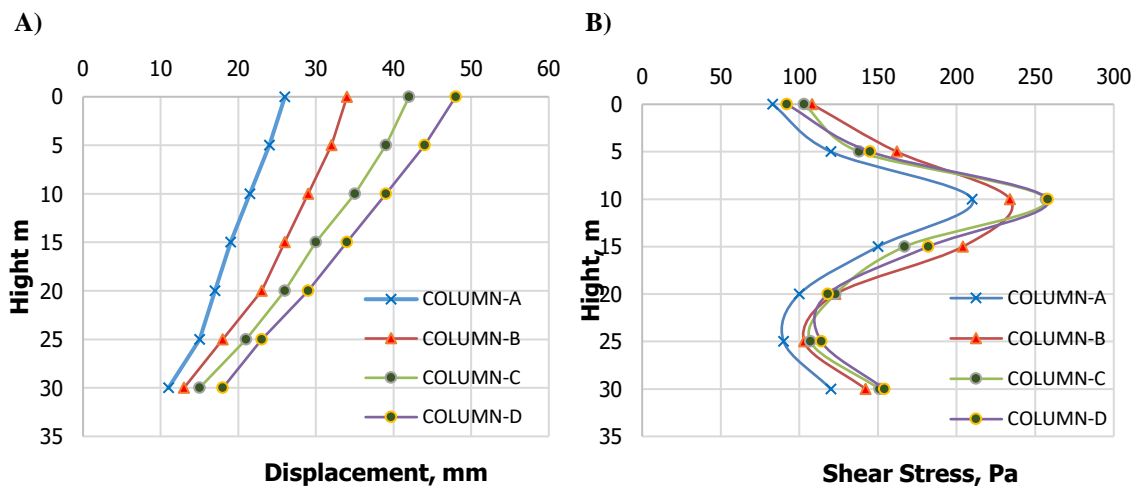


Figure (14). Seismic behavior of the column: A) the seismic displacement and B) shear stress

3.2.3. Seismic behavior of the Piles

The effect of the seismic load on the length of the steel pile is also investigated in terms of displacements, shear stresses, shear forces, and bending moments. Figures 15 illustrates the influence of a seismic load on the response of four corner piles (A, B, C, and D). According to Figure 15A, the displacements at the head of the piles are quite near. But there is a little shift in the displacements along one pile. This indicates that the pile head region is the area where the steel pipes are connected by beams. The displacements along the pile at a depth of about 15 meters are

relatively minimal, which indicates that the soil and the pile are interconnected. Thus, the piles at this depth show more resistance against the seismic loads. Based on Figure 15B, the shear stress at the top of piles A, C, and D is quite significant, and pile B has a value that is very near to pile C. All shear stress in piles is in the same direction. The shear stress along the piles is quite high at a depth of around 10 meters, indicating that the soil and the pile are interconnected.

Based on Figure 15C, it can be said that the shear force at the head of the piles is very large. Changes in shear force along the length of the pile occur at a depth of 13 meters below the ground surface. Also, the shear force along the piles is relatively tiny at a depth of around 30 meters.

The moments along the head of the piles are very significant, as seen in Figure 15D. It can also be seen that the variations in moments along pile length are inverted at 8 m below ground level for pile B and C, and at 17 m below ground level for pile A and D.

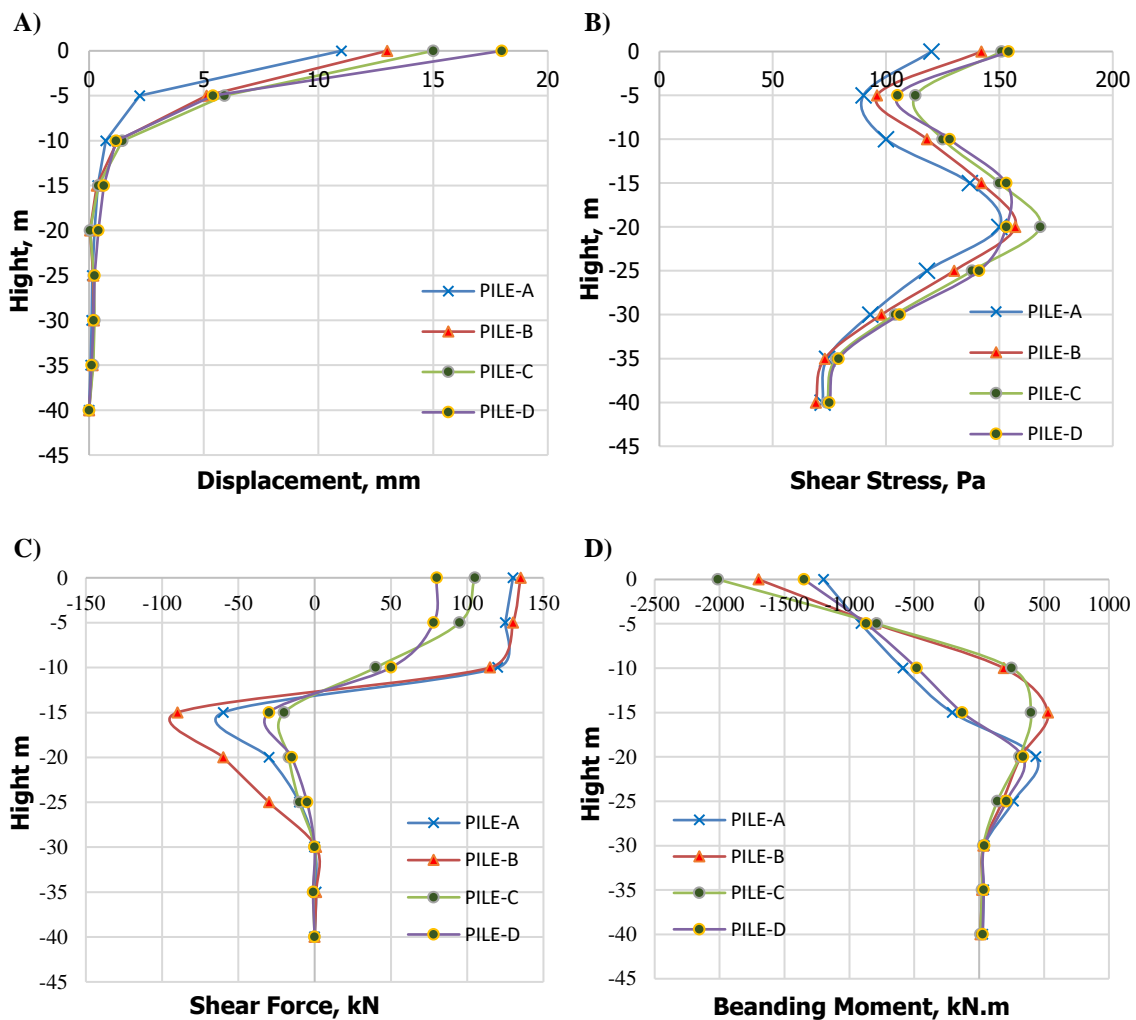


Figure (15). Seismic behavior of the Piles: A) seismic displacement; B) shear stress; C) shear force and D) bending moment

3.3. Behavior of dolphin structure under post-fire earthquake

The purpose of this investigation is to estimate the seismic response of the dolphin-type berth structure after exposure to various fire scenarios. In order to better examine the effects of temperature increase on the performance of the structure under post-fire earthquake, the fire is applied to the berth deck (first scenario) and near water surface (second scenario) in the first stage of loading.

3.3.1. Response of berth deck under post-fire earthquake

Figure 16 depicts the effect of a hydrocarbon fire on the seismic response of berth deck under applying the first and second fire scenarios. Regarding the influence of fire on the dolphin structure, which leads to a weakness in the stresses of steel and an increase in ductility, the deck displacement under post-fire earthquake is greater than the deck displacement under only earthquake record. So, it can be said that the deck displacement under post-fire earthquake in the second scenario is about 16% higher than in the first scenario. Also, the deck displacement under post-fire earthquake is about 15% and 27% higher than the seismic response of the berth deck under only earthquake loading in the first and second scenario, respectively.

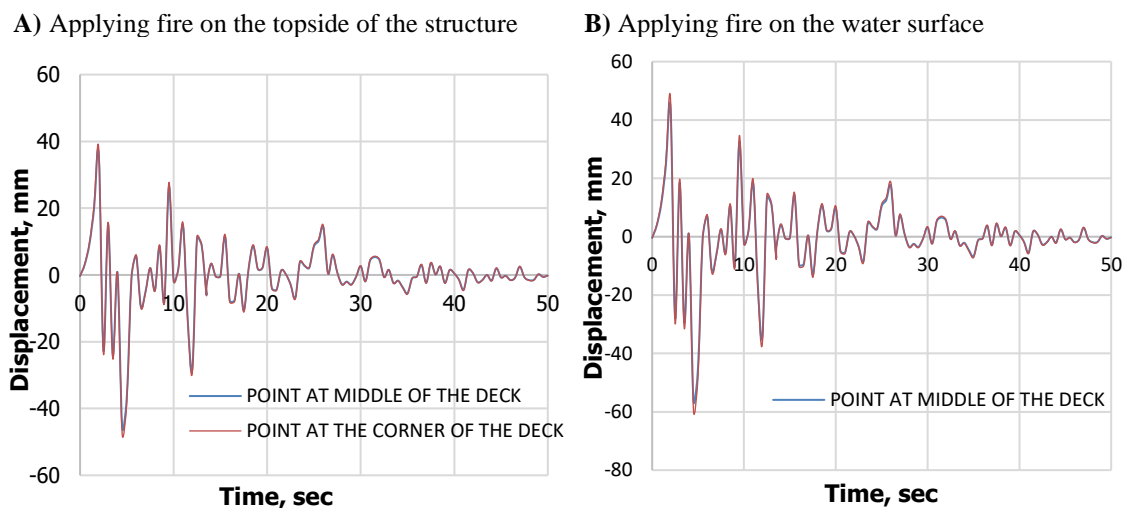


Figure (16). Response of berth deck under post-fire earthquake: A) first scenario and B) second scenario

3.3.2. Response of columns under post-fire earthquake

Figure 17 represents the effect of a hydrocarbon fire on the seismic response of columns A, B, C, and D in four corners. The results indicate an increase in the displacement of columns under post-fire earthquake loading. Therefore, it can be stated that the columns displacement under post-fire earthquake in the second scenario is about 13% higher than in the first scenario. Also, the columns displacement under post-fire earthquake is about 15% and 27% higher than the columns displacement under only earthquake loading in the first and second scenario, respectively.

Figure 18 illustrate the effect of the seismic load on the shear stress of columns (A, B, C, and D) after the structure was subjected to a hydrocarbon fire. The reactivity of the columns increases by 19

percent when the fire occurs on the near the water surface, compared to when the fire occurs on the topside of the dolphin structure. Considering the response of columns to earthquake loading, the rise of shear stress under post-fire earthquake is 16 percent and 32 percent in the first and second scenario, respectively.

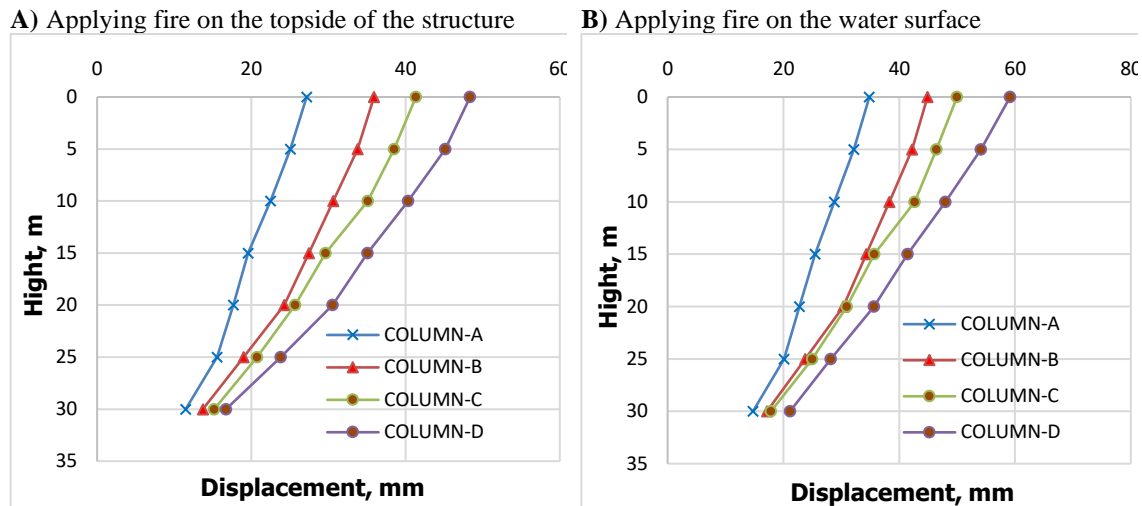


Figure (17). The seismic displacement of columns under post-fire earthquake loading: A) first scenario and B) second scenario

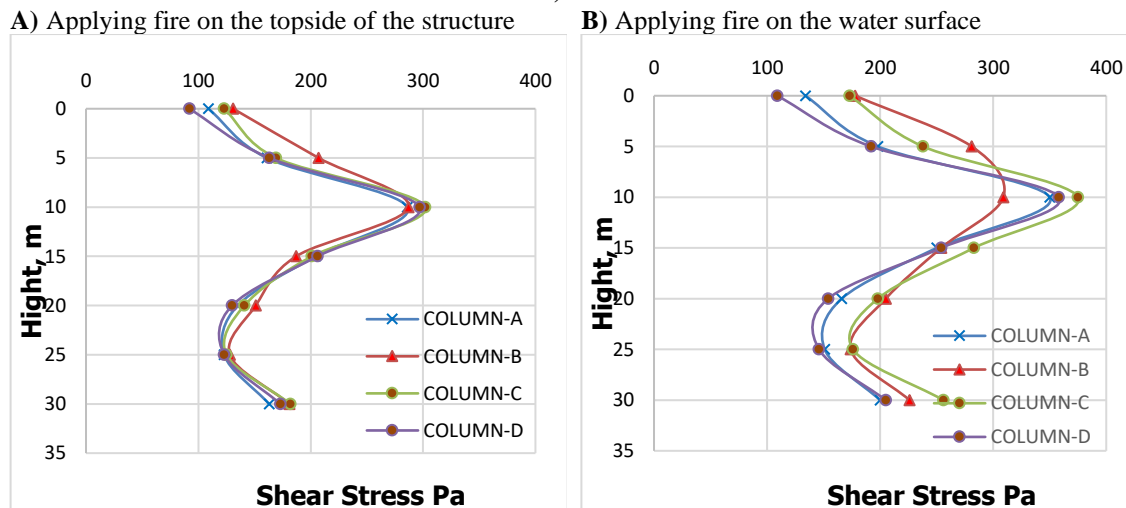


Figure (18). The shear stress of columns under post-fire earthquake loading: A) first scenario and B) second scenario

3.3.3. Response of piles under post-fire earthquake

Figure 19, demonstrate the influence of the seismic load on the response of steel offshore platform piles after applying hydrocarbon fire. The displacements at the head of piles have different values when compared to seismic loading. because the fire load modifies the characteristics of steel, whereas there is only a tiny variation in the displacements along one pile. The displacements along the piles are relatively minimal at a depth of around 10 meters, indicating that the soil and the pile are interconnected.

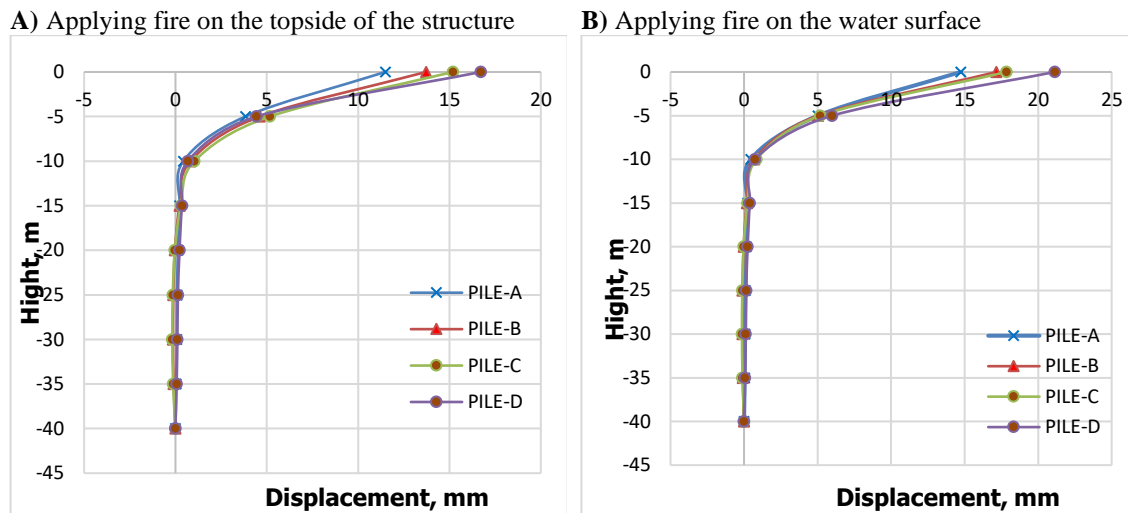


Figure (19). The seismic displacement of piles under post-fire earthquake loading: A) first scenario and B) second scenario

In comparison to the case of the seismic loading alone and due to the influence of the fire on the structure, an increase in shear stress is visible in the Figure 20. It's also worth mentioning that when a fire is near the water's surface, shear stress rises by 8% more than when the fire on the topside of the structure. The shear stress under the first and second scenario has increased by 8% and 14%, respectively, compared to the shear stress under seismic loading. At a depth of roughly 20 meters, the shear stress along the piles is rather significant, showing that the soil and the pile are interconnected.

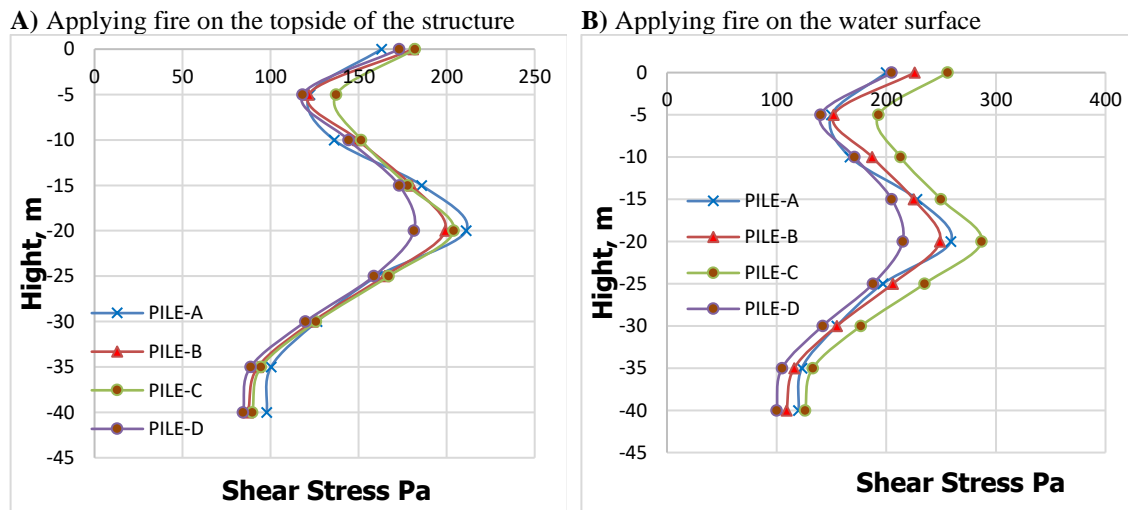


Figure (20). The shear stress of piles under post-fire earthquake loading: A) first scenario and B) second scenario

3.4. Bearing capacity and deformation performance

Changes in stiffness, bearing capacity and deformation performance for different loading conditions are reflected in the load - displacement and skeleton curve (Figure 21 and 22). According to the extracted curves, it can be stated that loading under the first scenario (Applying fire on the topside of the structure) creates more critical conditions for the structure (the structure's response is raised by 21%). Also, the bearing capacity of the structure in this case is less than other loading conditions.

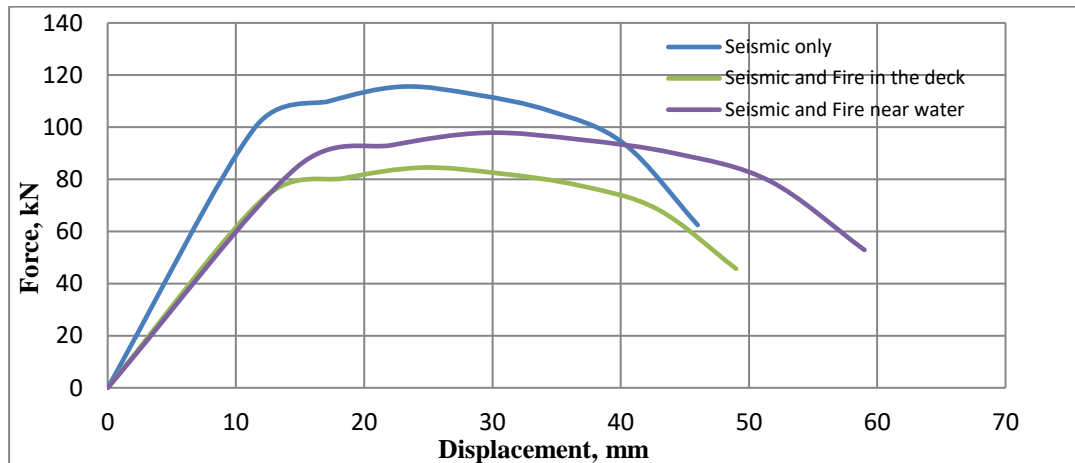
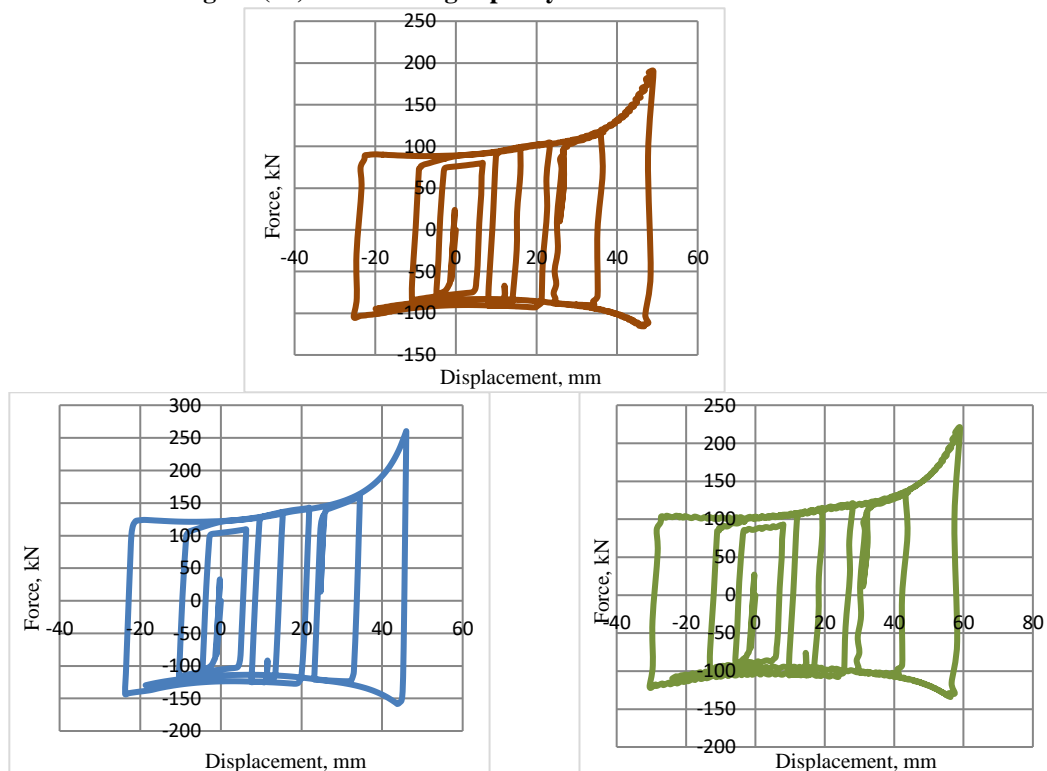


Figure (21). The bearing capacity of structure under three load cases



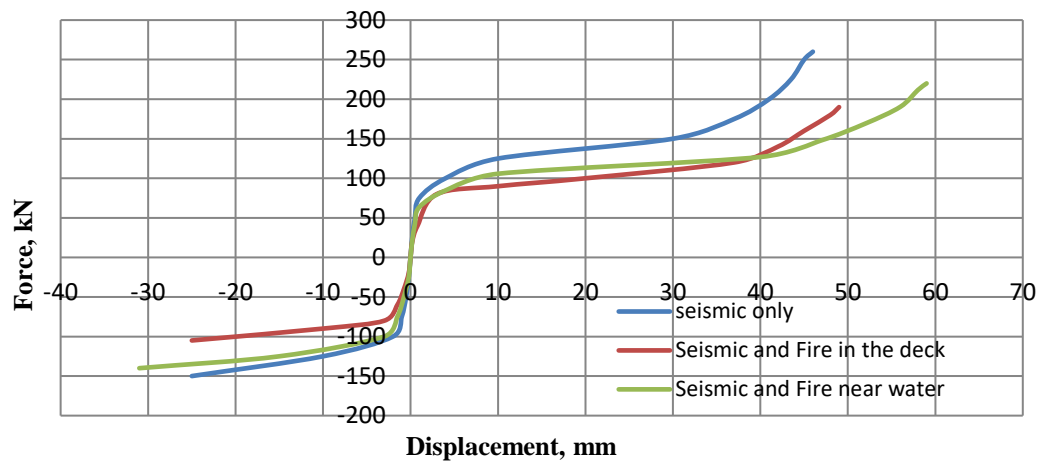


Figure (22). The Skeleton Curves for three load cases

4. Conclusion

The purpose of this investigation is to estimate the seismic response of the dolphin-type berth structure after exposure to various fire scenarios. In order to better examine the effects of temperature increase on the performance of the structure under post-fire earthquake, the fire is applied to the berth deck (first scenario) and near water surface (second scenario) in the first stage of loading. A summary of the results is presented as follows:

- the deck displacement under post-fire earthquake in the second scenario is about 16% higher than in the first scenario.
- Also, the deck displacement under post-fire earthquake is about 15% and 27% higher than the seismic response of the berth deck under only earthquake loading in the first and second scenario, respectively.
- the columns displacement under post-fire earthquake in the second scenario is about 13% higher than in the first scenario.
- Also, the columns displacement under post-fire earthquake is about 15% and 27% higher than the columns displacement under only earthquake loading in the first and second scenario, respectively.
- The reactivity of the columns increases by 19 percent when the fire occurs on the near the water surface, compared to when the fire occurs on the topside of the dolphin structure.
- Considering the response of columns to earthquake loading, the rise of shear stress under post-fire earthquake is 16 percent and 32 percent in the first and second scenario, respectively.
- The displacements at the head of piles have different values when compared to seismic loading, because the fire load modifies the characteristics of steel, whereas there is only a tiny variation in the displacements along one pile.
- The displacements along the piles are relatively minimal at a depth of around 10 meters, indicating that the soil and the pile are interconnected.
- It's also worth mentioning that when a fire is near the water's surface, shear stress rises by 8% more than when the fire on the topside of the structure.
- The shear stress under the first and second scenario has increased by 8% and 14%, respectively, compared to the shear stress under seismic loading. At a depth of roughly 20

meters, the shear stress along the piles is rather significant, showing that the soil and the pile are interconnected.

- Yield load is 120 kN for seismic only, 100 kN for fire near water and seismic and 80 kN for deck fire and seismic.

- According to the extracted curves, it can be stated that loading under the first scenario (Applying fire on the topside of the structure) creates more critical conditions for the structure (the structure's response is raised by 21%). Also, the bearing capacity of the structure in this case is less than other loading conditions.

References

1. Vazirizade SM, Azizsoltani H, & Haldar A. (2022). Reliability estimation of jacket type offshore platforms against seismic and wave loadings applied in time domain. *Ships and Offshore Structures*, 17(1): pp.143-152. <https://doi.org/10.1080/17445302.2020.1827632>
2. Hosseini F, Hokmabady H, Mojtahedi A, & Mohammadyzadeh S. (2019). seismic analysis of an offshore structure in Persian Gulf utilizing a physical model. *International Journal of Maritime Technology*, 11: pp.21-31.
3. Zheng SH, Zhang X, & Zhao X. (2018). Experimental investigation on seismic performance of corroded steel columns in offshore atmospheric environment. *The Structural Design of Tall and Special Buildings*, 28(2): e1580. DOI:10.1002/tal.1580
4. Asgarian B, Zarrin M, & Sabzeghabaian M. (2019). Effect of foundation behavior on steel jacket offshore platform failure modes under wave loading, *Ships and Offshore Structures*, 14(6). <https://doi.org/10.1080/17445302.2018.1526862>
5. Yang Y, Wu Q, He Z, Jia Z, & Zhang X. (2019). Seismic collapse performance of jacket offshore platforms with time-variant zonal corrosion model. *Applied Ocean Research*, 84: pp.268-278. <https://doi.org/10.1016/j.apor.2018.11.015>
6. Som A, & Das D. (2018). Seismic vibration control of offshore jacket platforms using decentralized sliding mode algorithm. *Ocean Engineering*, 152: pp.377-390. <https://doi.org/10.1016/j.oceaneng.2018.01.013>
7. Kavand A, Haeri SM, Raisianzadeh J, Sadeghi Meibodi A, & Afzal Soltani S. (2021). Seismic behavior of a dolphin-type berth subjected to liquefaction induced lateral spreading: 1g large scale shake table testing and numerical simulations. *Soil Dynamics and Earthquake Engineering*, 140: 106450. <https://doi.org/10.1016/j.soildyn.2020.106450>
8. Kaynia AM. (2021). Effect of kinematic interaction on seismic response of offshore wind turbines on monopoles. *Earthquake Engineering & Structural Dynamics*, 50(3): pp.777-790. <https://doi.org/10.1002/eqe.3371>
9. Kang HJ, Choi J, Lee D, & Park BJ. (2017). A framework for using computational fire simulations in the early phases of ship design. *Ocean Engineering*, 129: pp.335-342. <https://doi.org/10.1016/j.oceaneng.2016.11.018>
10. Manco MR, Vaz MA, Cyrino JCR, & Landesmann A. (2021). Thermomechanical performance of offshore topside steel structure exposed to localised fire conditions. *Marine Structures*, 76: 102924. <https://doi.org/10.1016/j.marstruc.2020.102924>
11. Patrizia B, Elena M, Alice S, et al., (2020). Simulation methodology for the assessment of the structural safety of concrete tunnel linings based on CFD fire – FE thermo-mechanical analysis: a case study. *Engineering Structures*, 225: 111193. <https://doi.org/10.1016/j.engstruct.2020.111193>

12. Moradi M, Tavakoli HR, & Abdollahzadeh G. (2019). Probabilistic assessment of failure time in steel frame subjected to fire load under progressive collapses scenario. *Engineering Failure Analysis*, 102: pp.136-147. <https://doi.org/10.1016/j.engfailanal.2019.04.015>
13. Soares CG, & Teixeira AP. (2000). Strength of plates subjected to localized heat loads. *Journal of Constructional Steel Research*, 53: pp.335-358. [https://doi.org/10.1016/S0143-974X\(99\)00045-0](https://doi.org/10.1016/S0143-974X(99)00045-0)
14. Azari-Dodaran N, & Ahmadi H. (2019). Structural behavior of right-angle two-planar tubular TT-joints subjected to axial loadings at fire-induced elevated temperatures, *Fire Safety Journal*, 108: 102849. <https://doi.org/10.1016/j.firesaf.2019.102849>
15. Xu J, Tong Y, Han J, Han Z, & Li Z. (2019). Fire resistance of thin-walled tubular T-joints with internal ring stiffeners under post-earthquake fire. *Thin-Walled Structures*, 145, 106433. <https://doi.org/10.1016/j.tws.2019.106433>
16. Ekmekyapar T, & Alhatmey IAH. (2019). Post-fire resistance of internally ring stiffened high-performance concrete-filled steel tube columns. *Engineering Structures*, 183: pp.375-388. <https://doi.org/10.1016/j.engstruct.2019.01.024>
17. Xiong MX, & Richard JYL. (2020). Buckling behavior of circular steel tubes infilled with C170/185 ultra-high-strength concrete under fire. *Engineering Structures*, 212: 110523. <https://doi.org/10.1016/j.engstruct.2020.110523>
18. Liu M, Zhao JC, & Jin M. (2010). An experimental study of the mechanical behavior of steel planar tubular trusses in a fire. *Journal of Constructional Steel Research*, 66(4): pp.504-511. <https://doi.org/10.1016/j.jcsr.2009.11.005>
19. Lien KH, Chiou YJ, Wang RZ, & Hsiao PA. (2010). Vector Form Intrinsic Finite Element analysis of nonlinear behavior of steel structures exposed to fire. *Engineering Structures*, 32: 80–92.
20. Moaveni S. (1999). *Finite Element Analysis Theory and Application with ANSYS* Prentice Hall, Inc., Upper Saddle River, New Jersey 07458, USA, PP. 447.
21. European Committee for Standardization (2005) EN 1993-1-1 Eurocode 3: Design of Steel Structures Part 1-1 General Rules and Rules for Buildings.
22. Buchanan AH, *Fire Engineering Design Guide*, Publisher Centre for Advanced Engineering, University of Canterbury (2001). <http://hdl.handle.net/10092/11531>



© 2023 by the authors. Licensee SCU, Ahvaz, Iran. This article is an open access article distributed under the terms and conditions of the Creative Commons Attribution 4.0 International (CC BY 4.0 license) (<http://creativecommons.org/licenses/by/4.0/>).

